Physics Letters A 381 (2017) 2743–2747

Contents lists available at ScienceDirect

Physics Letters A

www.elsevier.com/locate/pla

Difficulty of long-standing n-type conductivity in equilibrium and non-equilibrium γ-CuCl: A first-principles study

Dan Huang [a,c], Jin-Peng Xu [a], Jing-Wen Jiang [a], Yu-Jun Zhao [b,*], Biao-Lin Peng [a], Wen-Zheng Zhou [a,c], Jin Guo [a,c,*]

[a] Guangxi Key Laboratory for Relativistic Astrophysics, Guangxi Colleges and Universities Key Laboratory of Novel Energy Materials and Related Technology, Guangxi Novel Battery Materials Research Center of Engineering Technology, School of Physical Science and Technology, Guangxi University, Nanning 530004, PR China

[b] Department of Physics and State Key Laboratory of Luminescent Materials and Devices, South China University of Technology, Guangzhou 510640, PR China

[c] Guangxi Collaborative Innovation Center of Structure and Property for New Energy and Materials, School of Material Science and Engineering, Guilin University of Electronic Technology, Guilin, PR China

ARTICLE INFO

Article history:
Received 12 March 2017
Received in revised form 6 June 2017
Accepted 12 June 2017
Available online 16 June 2017
Communicated by R. Wu

Keywords:
Doping asymmetry
γ-CuCl
Defect formation energy
Defect diffusion barrier
Band edge position

ABSTRACT

Doping asymmetry is a pervasive issue in wide band gap semiconductors. We demonstrated that γ-CuCl is one of them with an intrinsic p-type semiconductor by first-principles calculations. The valence band maximum of γ-CuCl is dominated by the antibonding state of Cu-3*d* and Cl-3*p*, resulting in a high energy position. We further find that Cu vacancy has a relatively low diffusion barrier in addition to its low formation energy, implying that the long-standing n-type conductivity is hard to realize in γ-CuCl even with non-equilibrium approaches.

1. Introduction

Owing to their promising applications in ultra-violet (UV) optoelectronic devices, such as light-emitting diodes, laser diodes, detectors etc., wide-band-gap (WBG) semiconductor materials, such as zinc oxide (ZnO), gallium nitride (GaN), have been widely studied for many years [1–4]. Although a series of blue and UV devices have been fabricated by using GaN and ZnO, the growth of single crystal GaN layers is still a difficult work because of the shortage of high quality non-polar and low-cost substrates lattice matching GaN [5]. The available lattice-mismatched substrates, typically SiC or α-Al_2O_3 (sapphire), often resulting in the generation of misfit dislocations, are detrimental to the performance of related devices [5]. Furthermore, ZnO is usually growth intrinsically as a n-type semiconductor material [6]. Unfortunately, due to the doping asymmetry problem, it has proven difficult for ZnO to achieve high p-type doping [7] which is essential for the device implementation.

In order to open up new avenues in device applications, it is delightful to obtain n- and p-type films from the same semiconductor materials to form a high-quality homo-junction. However, a severe doping asymmetry problem has been suffered to the most WBG semiconductors experience, *i.e.*, they can be readily doped either n-type or p-type, but not both [8,9], because WBG semiconductors either have a low conduction-band minimum (CBM) or a high valence-band maximum (VBM) with reference to the vacuum level. Like the materials with an O-2*p* dominated VBM (i.e. ZnO, SnO_2 *etc.*), which is low relative to the vacuum level, excellent n-type conductivity has been achieved on ZnO:Al [6] and SnO_2:F [10] *etc.* However, great efforts have been devoted and long-term p-type stabilities are still hard to realize on them. By investigating the nature of extrinsic and intrinsic p-type defects in SnO_2 through a hybrid density functional study, Scanlon and Watson [11] demonstrated that a high-performance p-type SnO_2 cannot be achieved.

Recently, γ-CuCl as an efficient candidate for UV optoelectronics device has drawn much attention [12–23] because it is a zinc-blende direct band gap (3.39 eV) semiconductor and has a large exciton binding energy (190 meV) with its lattice constant closely matched to that of Si (<0.4%). The excitonic binding energy of γ-CuCl is much higher than that of GaN (20 meV), ZnO (63 meV) [17] and other related direct band gap inorganic materi-

* Corresponding authors.
E-mail addresses: zhaoyj@scut.edu.cn (Y.-J. Zhao), guojin@gxu.edu.cn (J. Guo).

http://dx.doi.org/10.1016/j.physleta.2017.06.020
0375-9601/

als. The hole conductivity in γ-CuCl has been reported by different groups due to the presence of Cu vacancies [14,15,24,25]. However, the p-type conductance is just at the order of 10^{-7} S·cm^{-1} [14,15]. By using the non-equilibrium process like the pulsed DC magnetron sputtering method [21,22], the n-type conductivity with a large electron concentration at 9.8×10^{18} cm^{-3} has also been reported [21] in Zn doped CuCl. In light of the experimental results, γ-CuCl seems like it can realize both the n-type and p-type doping and does not suffer the doping asymmetry problem. To above-mentioned situations, it is worthy to analyze the electronic structure and discuss the doping asymmetry in γ-CuCl.

In this letter, using first-principles calculations, we have studied the density of states (DOS), the bonding character, the carrier effective masses m^*, as well as the band edge positions ΔE_V and ΔE_C of γ-CuCl. Our calculated defect formation energies reveal that the p-type defect Cu vacancy (V_{Cu}) has low formation energy under all equilibrium growth conditions, especially when the Fermi energy level shifts to CBM. Our results also show V_{Cu} has a small diffusion barrier and a large diffusion coefficient in γ-CuCl. Therefore, V_{Cu} can compensate n-type conductivity achieved by non-equilibrium Zn doping in γ-CuCl, and thus the long-standing n-type stability is hard to realize in this compound.

2. Computation details

Our first-principles calculations were performed with the density functional theory (DFT) as implemented in the Vienna Ab-initio Simulation Package (VASP) [26]. The Perdew–Burke–Ernzerh (PBE) type of generalized gradient approximation (GGA) [27] was used with additional on-site Coulomb corrections (i.e., GGA + U) for the exchange correlation functional. The effective U values (5.2 and 6.5 eV for Cu-3*d* and Zn-3*d* states, respectively) were adopted following earlier studies [28,29]. The projector augmented wave method [30] are used to describe the interactions between the core electrons and the valence electrons. A 500 eV was used for the energy cutoff throughout the calculations. The Brillouin zone integrations were sampled with the Γ-centered $6 \times 6 \times 6$ Monkhorst–Pack meshes [31] for the unit cell. For the defect formation energy calculations, the Γ-centered $3 \times 3 \times 3$ mesh was used for the $2 \times 2 \times 2$ supercells (∼64 atoms). For the band offset calculations, the Γ-centered $6 \times 6 \times 1$ mesh was used for the A (4 unit cell layers) and B (4 unit cell layers) superlattice changing along (001) direction (64 atoms). The details for the formation energy calculations including the corrections and for the band offset calculations were described in our previous paper [32,33]. The calculations of diffusion paths and corresponding energy barriers are based on the nudged elastic band (NEB) method [34] in a $2 \times 2 \times 2$ supercell (∼64 atoms) with GGA + U lattice constants. In order to analyze the chemical bonding characters, the orbital interactions and crystal orbital overlap population (COOP) were obtained by using the Lobster program [35,36].

3. Results and discussions

Our calculated lattice constants are $a = b = c = 5.436$ Å, which are in agreement with the experimental data [37] $a = b = c = 5.42$ Å. Fig. 1a shows the partial density of state (PDOS) from the GGA + U calculation. From −5.5 to −4.0 eV with reference to VBM, the lower valence bands are contributed by Cu-3*d* state and Cl-3*p* state, and the upper valence bands (*i.e.* from −2.5 to −0 eV) are dominated by Cu-3*d* state with a slight contribution from Cl-3*p* state. In addition, there is an overlap around −5.2 eV between the peak of Cu-4*s* and Cl-3*p*. The lower conduction band is mainly made of Cu-4*s* and Cl-3*p*. Fig. 1b presents the COOPs of CuCl. The COOPs add the overlap dimension by showing the antibonding

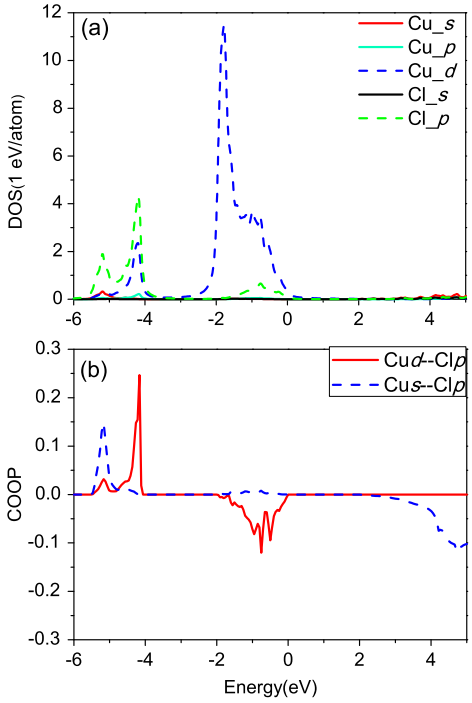

Fig. 1. The partial density of states (a) and the COOP (b) in γ-CuCl. The valence band maximum is set to zero.

(COOP < 0), non-bonding (COOP = 0) or bonding (COOP > 0) character of each electronic state over the system's chemical bonds. Combining with the DOSs and COOPs, we can speculate that the VBM comes from the antibonding state of Cu-3*d* and Cl-3*p* and the CBM comes from the antibonding state of Cu-4*s* and Cl-3*p*. The bonding state of Cu-3*d* and Cl-3*p* locates around −5 to −4 eV and the bonding state of Cu-4*s* and Cl-3*p* coincides with the overlap of Cu-4*s* and Cl-3*p* around −5.2 eV. Owing to the VBM from the antibonding state of Cu-3*d* and Cl-3*p* and dominated by Cu-3*d* state, the energy level of VBM with respect to vacuum level would be mainly decided by the cation Cu other than the anion Cl.

Our calculated band structure of γ-CuCl indicates it has a direct band gap with 1.69 eV at the Γ point, which is smaller than the reported values 3.39 eV [22], due to the well-known gap underestimation of GGA even with the on-site Coulomb interactions. The carrier effective masses are determined from the energy eigenvalue at a series of defined **k**-points along the selected symmetry axes. The effective mass tensors $m^*(\mathbf{k})$ of the carriers are obtained by fitting the $E - \mathbf{k}$ diagram around the CBM or the VBM with a parabolic expression $m^*(\mathbf{k}) = \pm\hbar^2[\partial^2 E(\mathbf{k})/\partial\mathbf{k}^2]^{-1}$. As presented in Table 1, the values of the electron effective masses are small and isotropic, which are correlated with the delocalized Cu-4*s* state and Cl-3*p* state at CBM. For the hole effective masses, the mass tensor has a bigger value and demonstrates a much more anisotropic characteristics, which should be related to the localized state Cu-3*d* at the VBM and the bonding direction of the antibonding state between the Cu-3*d* and Cl-3*p*. Our calculated hole effective masses of γ-CuCl are heavier than that of γ-CuI [38]. It can be explained by the higher *p*-orbital energy levels of I than that of Cl, which can contribute more *p*-state and result in a more delocalized character at VBM.

In order to estimate the type of conductivity of γ-CuCl, we need to find out which kind of defects has low formation energy under certain conditions and is responsible for the conductivity. Fig. 2 shows the formation energies of the intrinsic defects and Zn-related defects in γ-CuCl under Cu-poor and Cu-rich conditions. The Cu-rich condition is corresponding to $\Delta\mu_{Cu} = 0$ and $\Delta\mu_{Cl} =$

Table 1
Calculated carrier effective masses along different axes in γ-CuCl (unit: m_e).

	m_{001}	m_{011}	m_{111}
Holes	0.61	0.48	0.45
	1.41 (twofold)	1.41	2.80 (twofold)
		5.43	
Electrons	0.30	0.31	0.31

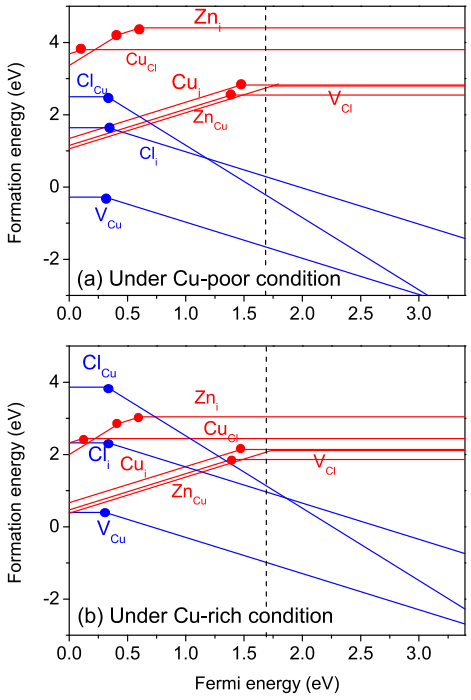

Fig. 2. Formation energy of intrinsic defects and extrinsic Zn-related defects in γ-CuCl under two different chemical potential conditions, *i.e.* Cu-poor (a) and Cu-rich (b). Red and blue lines represent the donor and acceptor defects, respectively. Here the experimental band gap [22] of γ-CuCl $E_g = 3.39$ eV is adopted. The vertical dashed line represents our calculated band gap.

ΔH(CuCl), while Cu-poor condition is assumed to $\Delta\mu_{Cl} = 0$ and $\Delta\mu_{Cu} = \Delta H$(CuCl). $\Delta\mu_{Zn}$ is the maximum Zn chemical potential under the condition of $\Delta\mu_{Zn} + 2\Delta\mu_{Cl} \leq \Delta H(ZnCl_2)$. Here, ΔH(CuCl) and $\Delta H(ZnCl_2)$ are the calculated formation enthalpies of CuCl and $ZnCl_2$. Our calculated enthalpies of γ-CuCl and $ZnCl_2$ are -1.29 eV and -3.96 eV, respectively, which are consistent with the experimental value of -1.42 eV and -4.30 eV [39]. The calculated acceptor transition level of V_{Cu} is 0.31 eV, which indicates that it is a p-type defect with relatively deep transition level. Other p-type defects like interstitial Cl (Cl_i) and Cl substituting Cu (Cl_{Cu}) have much larger formation energy than that of V_{Cu}, and thus they cannot contribute to p-type conductivity effectively. Our results confirmed that the p-type conductivity originates from the V_{Cu} since it has the lowest formation energy even under Cu-rich condition. However, the formation energy of V_{Cu} is also slightly less than zero near VBM under Cu-poor condition, which give rise to an unphysical meaning. Nagoya et al. [40] reported in another p-type semiconductor Cu_2ZnSnS_4 that the formation energy of V_{Cu} would raise with the increasing of V_{Cu} concentration. This means that the V_{Cu} in γ-CuCl could be also thermodynamically stable up under Cu-poor condition after reaching to a fairly high concentration. If assuming 5% concentration of V_{Cu} in γ-CuCl and then using the Boltzmann distribution law, the calculated hole concentrations are 8.3×10^{15} cm^{-3} under room temperature by adopting our calculated thermal ionization energies of V_{Cu} (0.31 eV), which is in agreement with the reported low p-type conductance ($\sim 10^{-7}$ S cm^{-1}) from experiment. Therefore, the low p-type conductance of γ-CuCl should be ascribed to the relatively deep acceptor transition level of V_{Cu}, other than high formation energy of p-type defects, or the possible n-type compensating defects.

For the n-type defects, the transition levels of Cu_i, Cu_{Cl} and Zn_{Cu} are 0.22 eV, 0.30 eV below the calculated CBM and 0.05 eV above the calculated CBM, respectively. The results indicate that Zn_{Cu} can supply an electron to the conduction band effectively owing to its transition level inside the conduction band. However, it has relatively high formation energies under equilibrium condition. By using the non-equilibrium process like the pulsed DC magnetron sputtering [21,22], the growth of Zn-doped CuCl can break up the equilibrium state and achieve a large n-type Zn_{Cu} concentration. Since Zn_{Cu} can supply the electrons effectively, the electron concentration can reach to a high value and the Fermi energy level will move close to the CBM in the as-grown samples, which is consistent with the large electron concentration (9.8×10^{18} cm^{-3}) from the experimental report [21]. When the sample became n-type and the Fermi energy level stayed close to CBM, the defect formation energy of V_{Cu} will decrease to negative value both under Cu-rich and Cu-poor condition. It means that Cu vacancies would be formed spontaneously and may result in a compensation on electron carrier concentration gradually. Here, we pointed out that GGA or GGA + U calculations severely underestimate the band gap, however, the error on the defect formation energy may alleviate in many systems [38,41]. For instance, although GGA, GGA + U and HSE presented different band gap values, the sequences on the defect formation energies for various defects in CuI [38] and GaN [41] systems from different functional calculations are consistent. Therefore, the tendency on the comparison of defect formation energies between V_{Cu} and Zn_{Cu} should be reliable although our GGA + U calculation underestimates the band gap. In addition, for the defect transition levels, Lany and Zunger [42] suggest that the shallow perturbed-host state should be moved with the conduction band and the deep defect-localized state should be kept in the band gap after the revision on the band edge position. It should be still a shallow donor-type defect for Zn_{Cu} and a deep acceptor-type defect for V_{Cu} from the calculations with more accurate band gap.

In order to evaluate the possibility of the carrier compensation in Zn-doped CuCl, we have discussed the binding energy between the n-type defect Zn_{Cu} and p-type defect V_{Cu} and the diffusion barriers of these defects. The binding energy of the defect complex ($Zn_{Cu} + V_{Cu}$) is calculated by $E_b = (E_{complex} + E_{pure}) - (E_{Zn_{Cu}} + E_{V_{Cu}})$ [43], where $E_{complex}$ is the energy of the supercell containing the defect complex, E_{pure} is the energy of the intrinsic supercell, and $E_{Zn_{Cu}}$, $E_{V_{Cu}}$ are the energies of the structures that only contain Zn_{Cu} or V_{Cu}. Our calculated binding energy for ($Zn_{Cu} + V_{Cu}$) is -2.27 eV, which indicates the n-type Zn_{Cu} and p-type V_{Cu} have a tendency to form a cluster. The formation of the neutral defect complex ($Zn_{Cu} + V_{Cu}$) indicates the electron carrier concentration from Zn_{Cu} will be balanced by the p-type defect V_{Cu}. The calculated diffusion barriers (Fig. 3) from a centered tetrahedron site to a nearby centered site for Zn_{Cu} and V_{Cu} are 0.63 eV and 0.38 eV, respectively. The diffusion barrier of V_{Cu} in CuCl is close to that of Na_{Cu} (0.36 eV) in Cu(In,Ga)Se_2, which is suggested as a faster diffusor in bulk Cu(In,Ga)Se_2 [44]. A rough diffusion coefficient of V_{Cu} can be determined according to the equation $D = a^2 \cdot \nu \cdot e^{(-E_A/kT)}$ [45,46], where a stands for the hopping distance of a diffusion, ν stands for the attempt frequency and E_A is taken from our calculated diffusion barrier of V_{Cu}, and kT is Boltzmann's constant times the temperature. In this calculation, a typical value of 10^{13} s^{-1} [46,47] was used for ν, and the temperature was set to be 300 K. The estimated diffusion coefficient of V_{Cu} is in the order of 6×10^{-9} cm^2 s^{-1}, which is much larger than that ($\sim 10^{-12}$ cm^2 s^{-1}) of Li ion [48,49] in the famous Li-ion battery cathode $LiCoO_2$. The small diffusion barrier and large diffu-

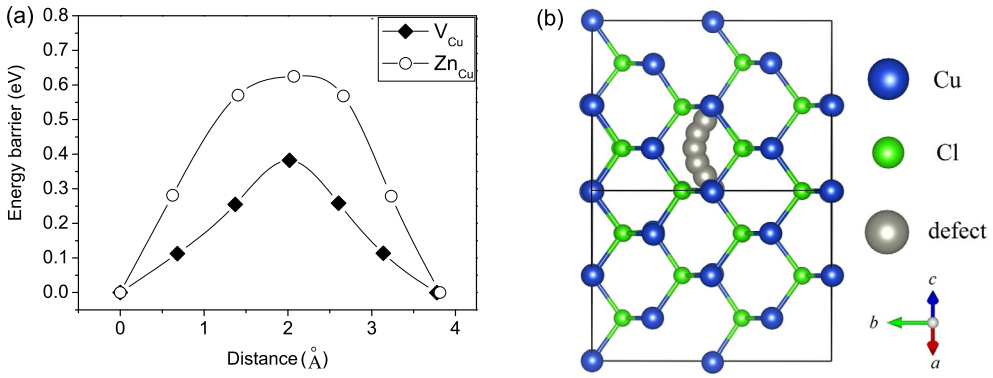

Fig. 3. The calculated diffusion barriers (a) of V_{Cu} and Zn_{Cu} from a centered tetrahedron site to a nearby centered site in γ-CuCl and the diffusion path (b) in our used supercell.

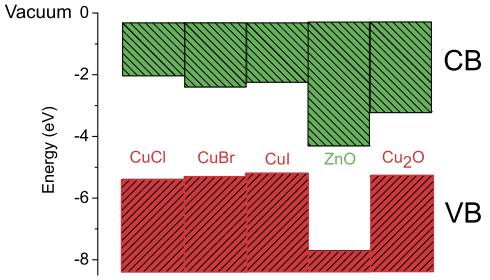

Fig. 4. The band offsets among CuCl, CuBr, CuI, ZnO and Cu_2O. The vacuum level is set to 0 eV. Here the experimental band gap of CuCl (3.39 eV, see Ref. [22]), CuBr (2.91 eV see Ref. [12]), CuI (2.95 eV see Ref. [12]), ZnO (3.4 eV see Ref. [51]) and Cu_2O (2.1 eV see Ref. [52]) are adopted. The ionization potentials of CuI (5.2 eV), ZnO (7.7 eV), and Cu_2O (5.3 eV), are taken from the literature see Refs. [50–52].

sion coefficient of V_{Cu} indicate that it can diffuse close to Zn_{Cu} and form a neutral defect complex with Zn_{Cu} after its spontaneous formation. These results demonstrate the intrinsic p-type defect V_{Cu} can compensate the n-type conductivity effectively and the n-type conductivity in the as-grown Zn-doped CuCl should be instable. Therefore, like other WBG semiconductors (ZnO, SnO_2 *etc.*), γ-CuCl also encounters a doping-asymmetry problem [8,9] and is hard to realize n-type with a long-term stability.

In order to illustrate the origin of the doping-asymmetry in γ-CuCl, we have investigated the band edge positions of CuCl and compared them with those from the n-type and p-type prototype compounds (i.e. ZnO for n type and Cu_2O for p-type). For the purpose of obtaining the band edge positions of CuCl relative to vacuum, we adopt the ionization potential of CuI (5.2 eV) from experiment [50], and then calculate the band offsets among CuCl, CuBr and CuI. Fig. 4 presents the band edge positions and band offsets among CuCl, CuBr, CuI, ZnO and Cu_2O. Our calculated results show that the valence band edge (−5.39 eV vs. vacuum) of CuCl is just lower than that of CuBr with 0.09 eV and that of CuI with 0.19 eV. Naturally, the band offset obtained from the superlattice model does not depends on the orientation of the interface. As a confirmation, here we have calculated the band offset from the superlattice oriented along (110) direction (96-atoms supercell). Our results show that the valence band offset of CuBr and CuI with CuCl are 0.09 and 0.20 eV, respectively, which is almost the same with the results from (001) oriented supercell. Our results demonstrate that this group compounds (i.e. CuCl, CuBr and CuI) almost have the same valence band positions. From our DOS and COOP analysis, it can be explained by the VBMs of these three Cu-based compounds mainly come from the 3*d* state of the same cation Cu and then have the similar valence band edge positions. The p-type conductivity has also been reported in CuI [53] and CuBr [54] experimentally. Based on a recently accepted doping limit rule [55], p-type doping can be achieved readily in semiconductor compounds with high VBM and n-type doping can be realized easily in semiconductor compounds with low CBM. This is the reason why the doping asymmetry exists in the WBG semiconductor, which cannot have a high VBM and low CBM at the same time. As a comparison with the band edge positions of the n-type prototype semiconductor ZnO and p-type prototype semiconductor Cu_2O, we found that CuCl has a similar VBM position with Cu_2O and has a much higher CBM position than ZnO, which suggests that γ-CuCl is an intrinsic p-type semiconductor and possesses a doping asymmetry problem [8,9].

4. Conclusions

In summary, our results reveal that the VBM of CuCl comes from the antibonding state of Cu-3*d* and Cl-3*p* with the majority from Cu-3*d* state. Based on the calculation on defect formation energy, we find that the p-type defect V_{Cu} always has the lowest formation energy under all chemical equilibrium conditions and γ-CuCl should be an intrinsic p-type semiconductor. With the Fermi level moving to n-type region, the formation energy of V_{Cu} will decrease to below zero and then it can be self-formation. Combining the self-formation with the small diffusion barrier and large diffusion coefficient of V_{Cu}, we demonstrate that V_{Cu} can compensate the n-type conductivity from the non-equilibrium Zn-doping in CuCl. The long-term stability of n-type conductivity is hard to maintain. Compared to the band edge positions with other WBG semiconductors, γ-CuCl has both high VBM and high CBM positions, which can explain the doping asymmetry in this compound.

Acknowledgements

This work was financially supported by the National Natural Science Foundation of China (Grant Nos. 61664003, 51571065 and 11574088), the Natural Science Foundation of Guangxi Province (Grant No. 2014GXNSFCA118002), and the Scientific Research Foundation of Guangxi University (Grant No. XGZ130718).

References

[1] M.J. Chen, J.R. Yang, M. Shiojiri, ZnO-based ultra-violet light emitting diodes and nanostructures fabricated by atomic layer deposition, Semicond. Sci. Technol. 27 (2012) 074005.
[2] X. Du, Z. Mei, Z. Liu, Y. Guo, T. Zhang, Y. Hou, Z. Zhang, Q. Xue, A.Y. Kuznetsov, Controlled growth of high-quality ZnO-based films and fabrication of visible-blind and solar-blind ultra-violet detectors, Adv. Mater. 21 (2009) 4625–4630.
[3] B.J. Kim, C. Lee, Y. Jung, K.H. Baik, M.A. Mastro, J.K. Hite, C.R. Eddy Jr., J. Kim, Large-area transparent conductive few-layer graphene electrode in GaN-based ultra-violet light-emitting diodes, Appl. Phys. Lett. 99 (2011) 143101.

[4] L. Zhang, F. Zhao, C. Wang, F. Wang, R. Huang, Q. Li, Optoelectronic characteristics of UV photodetector based on GaN/ZnO nanorods pin heterostructures, Electro. Mater. Lett. 11 (2015) 682–686.

[5] O. Ambacher, Growth and applications of group III-nitrides, J. Phys. D, Appl. Phys. 31 (1998) 2653.

[6] P. Raghu, N. Srinatha, C.S. Naveen, H.M. Mahesh, B. Angadi, Investigation on the effect of Al concentration on the structural, optical and electrical properties of spin coated Al: ZnO thin films, J. Alloys Compd. 694 (2017) 68–75.

[7] S.B. Zhang, S.H. Wei, A. Zunger, Intrinsic n-type versus p-type doping asymmetry and the defect physics of ZnO, Phys. Rev. B 63 (2001) 075205.

[8] Y. Yan, S.H. Wei, Doping asymmetry in wide-bandgap semiconductors: origins and solutions, Phys. Status Solidi B 245 (2008) 641–652.

[9] S. Lany, J. Osorio-Guillén, A. Zunger, Origins of the doping asymmetry in oxides: hole doping in NiO versus electron doping in ZnO, Phys. Rev. B 75 (2007) 241203.

[10] F. Wu, X. Tong, Z. Zhao, J. Gao, Y. Zhou, P. Kelly, Oxygen-controlled structures and properties of transparent conductive SnO_2:F films, J. Alloys Compd. 695 (2017) 765–770.

[11] D.O. Scanlon, G.W. Watson, On the possibility of p-type SnO_2, J. Mater. Chem. 22 (2012) 25236–25245.

[12] D. Ahn, S.H. Park, Cuprous halides semiconductors as a new means for highly efficient light-emitting diodes, Sci. Rep. 6 (2016) 20718.

[13] D. Ahn, S.L. Chuang, High optical gain of I–VII semiconductor quantum wells for efficient light-emitting devices, Appl. Phys. Lett. 102 (2013) 121114.

[14] F.O. Lucas, A. Mitra, P.J. McNally, S. Daniels, A.L. Bradley, D.M. Taylor, D.C. Cameron, Evaluation of the chemical, electronic and optoelectronic properties of γ-CuCl thin films and their fabrication on Si substrates, J. Phys. D, Appl. Phys. 40 (2007) 3461.

[15] F.O. Lucas, P.J. McNally, S. Daniels, D.M. Taylor, Electrical properties of γ-CuCl thin films, J. Mater. Sci., Mater. Electron. 20 (2009) 144–148.

[16] D. Danieluk, A.L. Bradley, A. Mitra, L. O'Reilly, O.F. Lucas, A. Cowley, P.J. McNally, B. Foy, E. McGlynn, Optical properties of undoped and oxygen doped CuCl film on silicon substrates, J. Mater. Sci., Mater. Electron. 20 (2009) 76–80.

[17] M.M. Alam, F.O. Lucas, D. Danieluk, A.L. Bradley, K.V. Rajani, S. Daniels, P.J. McNally, Hybrid organic–inorganic spin-on-glass CuCl films for optoelectronic applications, J. Phys. D, Appl. Phys. 42 (2009) 225307.

[18] Y.T. Lin, J.W. Ci, W.C. Tu, W.Y. Uen, S.M. Lan, T.N. Yang, C.C. Shen, C.H. Wu, Fabrication of cuprous chloride films on copper substrate by chemical bath deposition, Thin Solid Films 591 (2015) 43–48.

[19] M.M. Alam, S. Daniels, P.J. McNally, Reduction of the impact of atmospheric ageing effects on spin coated γ-CuCl nanocrystalline hybrid films, Opt. Mater. 51 (2016) 5–8.

[20] L. O'Reilly, A. Mitra, F.O. Lucas, Gomathi Natarajan, P.J. McNally, S. Daniels, A. Lankinen, D. Lowney, A.L. Bradley, D.C. Cameron, Characterisation of n-type γ-CuCl on Si for UV optoelectronic applications, J. Mater. Sci., Mater. Electron. 18 (2007) 57–60.

[21] K.V. Rajani, F.O. Lucas, S. Daniels, D. Danieluk, A.L. Bradley, A. Cowley, M.M. Alam, P.J. McNally, Growth of n-type γ-CuCl with improved carrier concentration by pulsed DC sputtering: structural, electronic and UV emission properties, Thin Solid Films 519 (2011) 6064–6068.

[22] K.V. Rajani, S. Daniels, P.J. McNally, S. Krishnamurthy, Soft x-ray spectroscopic investigation of Zn doped CuCl produced by pulsed dc magnetron sputtering, J. Phys. Condens. Matter 25 (2013) 285501.

[23] L. O'Reilly, A. Mitra, G. Natarajan, O.F. Lucas, P.J. McNally, S. Daniels, D.C. Cameron, A.L. Bradley, A. Reader, Impact on structural, optical and electrical properties of CuCl by incorporation of Zn for n-type doping, J. Cryst. Growth 287 (2006) 139–144.

[24] A.V. Joshi, J.B. Wagner Jr., Electrochemical studies on single crystalline CuCl solid electrolyte, J. Electrochem. Soc. 122 (1975) 1071–1080.

[25] J. Rivera, L.A. Murray, P.A. Hoss, Growth of corpus chloride single crystals for optical modulators, J. Cryst. Growth 1 (1976) 171–176.

[26] G. Kresse, J. Hafner, Ab initio molecular dynamics for liquid metals, Phys. Rev. B 47 (1993) 558–561.

[27] J.P. Perdew, K. Burke, M. Ernzerhof, Generalized gradient approximation made simple, Phys. Rev. Lett. 77 (1996) 3865–3868.

[28] D.O. Scanlon, K.G. Godinho, B.J. Morgan, G.W. Watson, Understanding conductivity anomalies in CuI-based delafossite transparent conducting oxides: theoretical insights, J. Chem. Phys. 132 (2010) 024707.

[29] Schleife, C. Rödl, F. Fuchs, J. Furthmüller, F. Bechstedt, Optical and energy-loss spectra of MgO, ZnO, and CdO from ab initio many-body calculations, Phys. Rev. B 80 (2009) 035112.

[30] G. Kresse, D. Joubert, From ultrasoft pseudopotentials to the projector augmented-wave method, Phys. Rev. B 59 (1999) 1758–1775.

[31] H.J. Monkhorst, J.D. Pack, Special points for Brillouin-zone integrations, Phys. Rev. B 13 (1976) 5188–5192.

[32] D. Huang, Y.J. Zhao, Z.P. Ju, L.Y. Gan, X.M. Chen, C.S. Li, C.M. Yao, J. Guo, First-principles prediction of a promising p-type transparent conductive material $CsGeCl_3$, Appl. Phys. Express 7 (2014) 041201.

[33] D. Huang, C. Persson, Photocatalyst $AgInS_2$ for active overall water-splitting: a first-principles study, Chem. Phys. Lett. 591 (2014) 189–192.

[34] G. Henkelman, B.P. Uberuaga, H. Jónsson, A climbing image nudged elastic band method for finding saddle points and minimum energy paths, J. Chem. Phys. 113 (2000) 9901–9904.

[35] S. Maintz, V.L. Deringer, A.L. Tchougréeff, R. Dronskowski, Analytic projection from plane-wave and PAW wavefunctions and application to chemical-bonding analysis in solids, J. Comput. Chem. 34 (2013) 2557–2567.

[36] R. Dronskowski, P.E. Bloechl, Crystal orbital Hamilton populations (COHP): energy-resolved visualization of chemical bonding in solids based on density-functional calculations, J. Phys. Chem. 97 (1993) 8617–8624.

[37] S. Hull, D.A. Keen, High-pressure polymorphism of the copper (I) halides: a neutron-diffraction study to ~10 GPa, Phys. Rev. B 50 (1994) 5868–5885.

[38] D. Huang, Y.J. Zhao, S. Li, C.S. Li, J.J. Nie, X.H. Cai, C.M. Yao, First-principles study of γ-CuI for p-type transparent conducting materials, J. Phys. D, Appl. Phys. 45 (2012) 145102.

[39] D.R. Lide, CRC Handbook of Chemistry and Physics, 89th ed., CRC/Taylor and Francis, Boca Raton/London, 2009.

[40] A. Nagoya, R. Asahi, R. Wahl, G. Kresse, Defect formation and phase stability of Cu_2ZnSnS_4 photovoltaic material, Phys. Rev. B 81 (2010) 113202.

[41] J.L. Lyons, C.G. Van de Walle, Computationally predicted energies and properties of defects in GaN, NPJ Comput. Mater. 3 (2017) 12.

[42] S. Lany, A. Zunger, Assessment of correction methods for the band-gap problem and for finite-size effects in supercell defect calculations: case studies for ZnO and GaAs, Phys. Rev. B 78 (2008) 235104.

[43] D. Huang, C. Persson, Stability of the bandgap in Cu-poor $CuInSe_2$, J. Phys. Condens. Matter 24 (2012) 455503.

[44] Z.K. Yuan, S. Chen, Y. Xie, J.S. Park, H. Xiang, X.G. Gong, S.H. Wei, Na-diffusion enhanced p-type conductivity in $Cu(In,Ga)Se_2$: a new mechanism for efficient doping in semiconductors, Adv. Energy Mater. 6 (2016) 1601191.

[45] J. Wu, G. Gao, G. Wu, B. Liu, H. Yang, X. Zhou, J. Wang, $MgVPO_4F$ as a one-dimensional Mg-ion conductor for Mg ion battery positive electrode: a first principles calculation, RSC Adv. 4 (2014) 15014–15017.

[46] X. Lv, Z. Xu, J. Li, J. Chen, Q. Liu, Insights into stability, electronic properties, defect properties and Li ions migration of Na, Mg and Al-doped $LiVPO_4F$ for cathode materials of lithium ion batteries: a first-principles investigation, J. Solid State Chem. 239 (2016) 228–236.

[47] H. Kim, K.E. Kweon, C.Y. Chou, J.G. Ekerdt, G.S. Hwang, On the nature and behavior of Li atoms in Si: a first principles study, J. Phys. Chem. C 114 (2010) 17942–17946.

[48] Y.H. Rho, K. Kanamura, Li^+-ion diffusion in $LiCoO_2$ thin film prepared by the poly(vinylpyrrolidone) sol–gel method, J. Electrochem. Soc. 151 (2004) A1406–A1411.

[49] H. Xia, L. Lu, G.J. Ceder, Li diffusion in $LiCoO_2$ thin films prepared by pulsed laser deposition, J. Power Sources 159 (2006) 1422–1427.

[50] F.L. Schein, H.V. Wenckstern, M. Grundmann, Transparent p-CuI/n-ZnO heterojunction diodes, Appl. Phys. Lett. 102 (2013) 092109.

[51] A. Walsh, J. Buckeridge, C.R.A. Catlow, A.J. Jackson, T.W. Keal, M. Miskufova, P. Sherwood, S.A. Shevlin, M.B. Watkins, S.M. Woodley, A.A. Sokol, Limits to doping of wide band gap semiconductors, Chem. Mater. 25 (2013) 2924–2926.

[52] S.S. Wilson, Y. Tolstova, D.O. Scanlon, G.W. Watson, H.A. Atwater, Interface stoichiometry control to improve device voltage and modify band alignment in ZnO/Cu_2O heterojunction solar cells, Energy Environ. Sci. 7 (2014) 3606–3610.

[53] C. Yang, M. Kneiß, M. Lorenz, M. Grundmann, Room-temperature synthesized copper iodide thin film as degenerate p-type transparent conductor with a boosted figure of merit, Proc. Natl. Acad. Sci. USA 113 (2016) 12929–12933.

[54] K.V. Rajani, S. Daniels, M. Rahman, A. Cowley, P.J. McNally, Deposition of earth-abundant p-type CuBr films with high hole conductivity and realization of p-CuBr/n-Si heterojunction solar cell, Mater. Lett. 111 (2013) 63–66.

[55] S.B. Zhang, S.H. Wei, A. Zunger, Microscopic origin of the phenomenological equilibrium "doping limit rule" in n-type III–V semiconductors, Phys. Rev. Lett. 84 (2000) 1232–1235.